Study of two body hadronic decays $\Lambda_b \to \Lambda(p)P(V)$ in the instantaneous approximation of the Bethe-Salpeter equation approach

Y. Liu,* X.-H. Guo,† and C. Wang‡

College of Nuclear Science and Technology, Beijing Normal University, Beijing 100875, People's Republic of China

(Received 25 August 2014; revised manuscript received 10 November 2014; published 21 January 2015)

In this work, we study weak transitions of Λ_b to light baryons Λ and p in the Bethe-Salpeter equation approach. In the heavy quark limit, based on the picture that Λ_b is composed of a heavy b-quark and a light diquark, the Bethe-Salpeter equation for Λ_b was established in previous works. Although the light baryon $\Lambda(p)$ is composed of various quark-diquark configurations based on the $SU(6)$ spin-flavor wave functions, only the configuration $s(ud)_{0,0}$ $[u(ud)_{0,0}]$ [$(ud)_{0,0}$ is a scalar diquark composed of u and d quarks] contributes to $\Lambda_b \to \Lambda$ ($\Lambda_b \to p$) transition. We establish the Bethe-Salpeter equations for the systems $s(ud)_{0,0}$ and $u(ud)_{0,0}$ and calculate their Bethe-Salpeter wave functions in the covariant instantaneous approximation with the kernel containing both scalar confinement and one-gluon-exchange terms. Then, the form factors for $\Lambda_b \to \Lambda$ and $\Lambda_b \to p$ weak transitions are obtained with Bethe-Salpeter wave functions for Λ_b, Λ, and p. Consequently, we calculate the branching ratios of $\Lambda_b \to \Lambda P$, $\Lambda_b \to \Lambda V$, $\Lambda \to pP$, and $\Lambda_b \to pV$ (P and V denote pseudoscalar and vector mesons, respectively) in the factorization approach.

DOI: 10.1103/PhysRevD.91.016006 PACS numbers: 11.10.St, 12.39.Hg, 14.20.Lq, 14.20.Mr

I. INTRODUCTION

In recent years, much more new data about weak decays of Λ_b have appeared. For instance, the branching ratios of the semileptonic decay $\Lambda_b \to \Lambda_c l\nu$ [1] and the two body decay $\Lambda_b \to \Lambda_c^+ \pi^-$ [2] were measured. CDF and D0 measured the lifetime of Λ_b. Furthermore, the decay $\Lambda_b \to \Lambda J/\psi$ was observed by CDF, and the ratio of the cross section times the branching fraction, $\sigma_{\Lambda_b} \mathrm{B}(\Lambda_b \to \Lambda J/\psi)/\sigma_{B^0} \mathrm{B}(B^0 \to J/\psi K_s)$, was measured. The branching ratio of $\Lambda_b \to \Lambda J/\psi$ turns out to be $(3.7 \pm 1.7 \pm 0.4) \times 10^{-4}$ [3], assuming $\sigma_{\Lambda_b}/\sigma_B = 0.1/0.375$ and $B(B^0 \to J/\psi K_s) = 3.7 \times 10^{-4}$ [3,4]. $F(\Lambda_b) B(\Lambda_b \to \Lambda J/\psi)$ measured by D0 is $(6.01 \pm 0.60 \pm 0.58 \pm 0.28) \times 10^{-5}$ [5], where $F(\Lambda_b)$ is the fraction of the b-quark transition into Λ_b. In the past theoretical studies, people gave predictions for Λ_b decays by calculating transition form factors for Λ_b decays, assuming pole dominance for the form factors [6,7] or adopting models for describing baryon wave functions [8,9]. It is the aim of the present paper to study nonleptonic decays of Λ_b to light baryons Λ and p theoretically in the Bethe-Salpteter (BS) equation approach. These decays include $\Lambda_b \to \Lambda(p)P$, where the pseudoscalar meson P is π^-, K^-, or π^0, and $\Lambda_b \to \Lambda(p)V$, where the vector meson V is J/ψ, ρ^0, ρ^-, or K^*. Experimentally, $\Lambda_b \to p\pi^-$ and $\Lambda_b \to pK^-$ have been measured [4].

In the limit $m_b \to \infty$, with the application of heavy quark effective theory, $\Lambda_b \to \Lambda\,(p)$ transition can be described by two independent form factors [10]. The decrease in the number of form factors simplifies calculations. However, these two form factors contain all soft QCD effects that are difficult to calculate from first principles. Therefore, one must resort to some phenomenological models [6–8,11] to calculate them. In previous works, the form factors for $\Lambda_b \to \Lambda_c$ were calculated in the BS equation approach [12,13] within the "quark-diquark" model. Theoretical results for $\Lambda_b \to \Lambda_c$ semileptonic and nonleptonic decay widths were found to be consistent with experimental data. Furthermore, baryons containing a light quark and a heavy diquark ($\Omega_{QQ'}$, $\Xi_{QQ'}$) $(Q, Q' = b, c)$ were also studied in the BS equation formalism [14]. Since there have been experimental data for Λ_b to light baryon decays, we will extend the BS equation model to light baryons in the present work.

In the quark-diquark model, a baryon is regarded as a bound state of two particles: one is a quark, and the other is a quasiparticle made of two quarks, or diquark. For a heavy baryon containing a heavy quark or two heavy quarks, due to the flavor and spin symmetries $SU(2)_f \times SU(2)_s$ in the heavy quark limit, such a baryon can be regarded as composed of a heavy quark and a light diquark or a heavy diquark and a light quark. On the other hand, a light baryon composed of u, d, and s quarks is a much more complex system in which all the three light quarks play important roles in the dynamics of the baryon. Based on the $SU(6)$ spin-flavor wave functions, the light baryons Λ and p contain several quark-diquark configurations. However, only the configuration $s(ud)_{0,0}$ $[u(ud)_{0,0}]$ [the first and second subscripts correspond to the total spin and the third component of the spin of the (ud) diquark, respectively] contributes to $\Lambda_b \to \Lambda$ $(\Lambda_b \to p)$ transition. We will

*yingliubnu@gmail.com
†Corresponding author.
xhguo@bnu.edu.cn
‡chaowang07@lzu.edu.cn

establish the Bethe-Salpeter equations for the systems $s(ud)_{0,0}$ and $u(ud)_{0,0}$ and solve them in the covariant instantaneous approximation with the kernel containing both scalar confinement and one-gluon-exchange terms. The form factors for the heavy-light transitions will be expressed in terms of the BS wave functions obtained for the initial and final baryons. Finally, we will calculate the decay branching ratios for $\Lambda_b \to \Lambda$ and $\Lambda_b \to p$ plus a pseudosclar meson or a vector meson.

The remainder of this paper is organized as follows. In Sec. II, we will establish the BS equations for the systems containing a light quark and a light scalar diquark. The normalization conditions for the BS wave functions will also be given in this section. Then, the BS wave functions will be calculated numerically. In Sec. III, the form factors for $\Lambda_b \to \Lambda$ and $\Lambda_b \to p$ will be derived from the BS wave functions obtained in Sec. II. In Sec. IV, the branching ratios for $\Lambda_b \to \Lambda$ and $\Lambda_b \to p$ plus a pseudoscalar meson or a vector meson will be obtained. Section V will be reserved for a summary and some discussions.

II. BS EQUATION FOR A SYSTEM CONTAINING A LIGHT QUARK AND A LIGHT SCALAR DIQUARK

In general, the parity of a baryon at the ground state is positive. Since the parity of the quark in the baryon is supposed to be positive, the parity of the diquark involved in the ground state baryon should also be positive. Because of the Pauli principle, two quarks with same flavor constitute an axial-vector diquark. On the other hand, two quarks with different flavors can constitute a scalar diquark or an axial-vector diquark. Regarding Λ_b as a bound state of a light scalar diquark and a heavy b-quark, the BS equation for Λ_b has been studied extensively [15,16]. As discussed in Introduction, to study the weak transitions $\Lambda_b \to \Lambda$ and $\Lambda_b \to p$, we need to establish the BS equations of $q(ud)_{0,0}$ ($q = s$ or u). We define the BS wave function of the $q(ud)_{0,0}$ system as

$$\chi(x_1, x_2, P) = \langle 0|T\psi(x_1)\varphi(x_2)|P\rangle, \tag{1}$$

where $\psi(x_1)$ and $\varphi(x_2)$ are the field operators of the light quark at position x_1 and the light scalar diquark at position x_2, respectively; $P = Mv$ is the momentum of Λ or p; and M (v) is its mass (velocity). Let m_q and m_D represent the masses of the light quark and the light diquark in the baryon Λ or p; $\lambda_1 = \frac{m_q}{m_q+m_D}$, $\lambda_2 = \frac{m_D}{m_q+m_D}$, and p represent the relative momentum of the two constituents. $X = \lambda_1 x_1 + \lambda_2 x_2$ is the coordinate of the center of mass, and $x = x_1 - x_2$. Then, we define the BS wave function in momentum space:

$$\chi(x_1, x_2, P) = e^{iPX} \int \frac{d^4p}{(2\pi)^4} e^{ipx} \chi_P(p). \tag{2}$$

It is straightforward to prove that the BS equation for the $q(ud)_{0,0}$ system has the form in momentum space of

$$\chi_P(p) = S_F(p_1) \int \frac{d^4q}{(2\pi)^4} K(P, p, q) \chi_P(q) S_D(p_2), \tag{3}$$

where $p_1 = \lambda_1 P + p$ and $p_2 = \lambda_2 P - p$ are the momenta of the light quark q and the light scalar diquark, respectively; $K(P, p, q)$ is the kernel that is defined as the sum of two-particle-irreducible diagrams; and $S_F(p_1)$ and $S_D(p_2)$ are propagators of the light quark with momentum p_1 and the light diquark with momentum p_2. Motivated by the potential model, the kernel is given by [15,17]

$$-iK(P, p, q) = I \otimes IV_1(p, q) + \gamma_\mu \otimes \Gamma^\mu V_2(p, q), \tag{4}$$

where $\Gamma^\mu = (p_2 + q_2)^\mu F(Q^2)$ is the effective vertex of a gluon with two scalar diquarks and $F(Q^2)$ is used to describe the structure of the diquark [15,18]

$$F(Q^2) = \frac{\alpha_{\text{seff}} Q_0^2}{Q^2 + Q_0^2}, \tag{5}$$

where Q_0^2 is a parameter that freezes $F(Q^2)$ when Q^2 is very small. In the high-energy region, the form factor is proportional to $\frac{1}{Q^2}$, which is consistent with perturbative QCD calculations. By analyzing the electromagnetic form factor for the proton, it was found that $Q_0^2 = 3.2\ \text{GeV}^2$ [15,18] can lead to consistent results with the experimental data. V_1 and V_2 are the scalar confinement and one-gluon-exchange terms that have the forms in the covariant instantaneous approximation [14–16,19–21]

$$\tilde{V}_1(p_t - q_t) = \frac{8\pi\kappa}{[(p_t - q_t)^2 + \mu^2]^2} - (2\pi)^3 \delta^3(p_t - q_t) \int \frac{d^3k}{(2\pi)^3} \frac{8\pi\kappa}{(k^2 + \mu^2)^2}, \tag{6}$$

$$\tilde{V}_2(p_t - q_t) = -\frac{16\pi}{3} \frac{\alpha_{\text{seff}}}{(p_t - q_t)^2 + \mu^2}, \tag{7}$$

respectively, where p_t and q_t are the transverse projection of the relative momentum along the momentum P and are defined as $p_t^\mu = p^\mu - v \cdot p v^\mu$ and $q_t^\mu = q^\mu - v \cdot q v^\mu$. The second term of $\tilde{V}_1$ is introduced to remove the infrared singularity at the point $p_t = q_t$, and the small parameter μ is introduced to avoid the divergence in numerical calculations. The dimension of κ is 3, and that of κ' in the meson case is 2. The extra dimension in κ should be caused by nonperturbative QCD effects, and hence $\kappa \sim \Lambda_{\text{QCD}}\kappa'$ [17]. κ' is the confinement parameter in the heavy meson case and is about $0.2\ \text{GeV}^2$ [15], and Λ_{QCD} is the only parameter that is related to confinement. So the parameter κ may range

from 0.02 to 0.1 GeV^3. Furthermore, by studying the average momentum of the b quark in Λ_b and comparing it with this quantity derived from the experimental value of the average momentum of the b quark in the B meson with the aid of heavy quark effective theory, κ can be constrained to a narrower range: roughly from 0.02 to 0.08 GeV^3 [19]. Therefore, in our numerical calculations, the parameter κ is chosen to vary in the region between 0.02 and 0.08 GeV^3 [9,20]. The light quark propagator can be written in the form [14,21]

$$S_F(p_1) = i\not{v}\left[\frac{\Lambda_q^+}{\lambda_1 M + p_l - \omega_q + i\varepsilon} + \frac{\Lambda_q^-}{\lambda_1 M + p_l + \omega_q - i\varepsilon}\right], \tag{8}$$

where $p_l(= p\cdot v)$ and p_t^μ are the longitudinal and transverse projections of the relative momentum along the light baryon momentum, respectively; $\omega_q = \sqrt{m_q^2 - p_t^2}$; and $\Lambda_q^\pm$ are the projection operators given by

$$\Lambda_q^\pm = \frac{\omega_q \pm \not{v}(\not{p}_t + m_q)}{2\omega_q}. \tag{9}$$

The propagator of the scalar light diquark can be written as

$$S_D(p_2) = \frac{i}{(\lambda_2 M - p_l - \omega_D + i\varepsilon)(\lambda_2 M - p_l + \omega_D - i\varepsilon)}, \tag{10}$$

where $\omega_D = \sqrt{m_D^2 - p_t^2}$. In general, considering $\not{v}u(v,s) = u(v,s)$, where $u(v,s)$ is the spinor of Λ or p with helicity s, $\chi_P(p)$ can be expanded as

$$\chi_P(p) = (f_1 + f_2\gamma_5 + f_3\gamma_5\not{p}_t + f_4\not{p}_t + f_5\sigma_{\mu\nu}\varepsilon^{\mu\nu\alpha\beta}p_{t\alpha}v_\beta)u(v,s), \tag{11}$$

where f_i $(i = 1,\ldots,5)$ are the Lorentz-scalar functions of p_t^2 and p_l. After considering the constraints on $\chi_p(p)$ imposed by parity and Lorentz transformations, we simplify Eq. (11) to the following form:

$$\chi_P(p) = (f_1 + \not{p}_t f_2)u(v,s). \tag{12}$$

Defining $\tilde{f}_{1(2)} = \int \frac{dp_l}{2\pi} f_{1(2)}$, we find that the BS scalar wave functions satisfy the coupled integral equations as follows:

$$\begin{aligned}\tilde{f}_1(p_t) = &-\int \frac{d^3p_t}{(2\pi)^3}\frac{1}{4\omega_q\omega_D(M-\omega_q-w_D)}[(m_q+\omega_q)(\tilde{V}_1 + 2\omega_D\tilde{V}_2F(Q^2))\tilde{f}_1(q_t) - (p_t\cdot q_t + p_t^2)\tilde{V}_2F(Q^2)\tilde{f}_1(q_t)]\\ &-\int \frac{d^3p_t}{(2\pi)^3}\frac{1}{4\omega_q\omega_D(M-\omega_q-\omega_D)}[(\tilde{V}_1 - 2\omega_D\tilde{V}_2F(Q^2))p_t\cdot q_t\tilde{f}_2(q_t) - (m_q+\omega_q)(p_t\cdot q_t + q_t^2)\tilde{V}_2F(Q^2)\tilde{f}_2(q_t)],\end{aligned} \tag{13}$$

$$\begin{aligned}\tilde{f}_2(p_t) = &-\int \frac{d^3p_t}{(2\pi)^3}\frac{1}{4\omega_Q\omega_D(M-\omega_q-\omega_D)}\left[(\tilde{V}_1 + 2\omega_D\tilde{V}_2F(Q^2))\tilde{f}_1(q_t) - (m_q-\omega_q)\frac{(p_t\cdot q_t + p_t^2)}{p_t^2}\tilde{V}_2F(Q^2)\tilde{f}_1(q_t)\right]\\ &-\int \frac{d^3p_t}{(2\pi)^3}\frac{1}{4\omega_q\omega_D(M-\omega_q-\omega_D)}\left[(m_q-\omega_q)(\tilde{V}_1 - 2\omega_D\tilde{V}_2F(Q^2))\frac{p_t\cdot q_t}{p_t^2}\tilde{f}_2(q_t) - (p_t\cdot q_t + q_t^2)\tilde{V}_2F(Q^2)\tilde{f}_2(q_t)\right].\end{aligned} \tag{14}$$

The normalization condition for the BS wave function is given after imposing the covariant instantaneous approximation on the kernel as [14,21,22]

$$\begin{aligned}&i\delta^{i_1i_2}_{j_1j_2}\int \frac{d^4qd^4p}{(2\pi)^8}\bar{\chi}_P(p,s)\left[\frac{\partial}{\partial P_0}I_P(p,q)^{i_1i_2j_2j_1}\right]\chi_P(q,s')\\ &\quad = \delta_{ss'},\end{aligned} \tag{15}$$

where $i_{1(2)}$ and $j_{1(2)}$ represent the color indices of the light diquark and the light quark, respectively; $s^{(\prime)}$ is the spin index for the light baryon; $\delta^{i_1,i_2}_{j_1,j_2} = \delta^{i_1}_{j_1}\delta^{i_2}_{j_2} - \delta^{i_1}_{j_2}\delta^{i_2}_{j_1}$; and $I_P^{i_1i_2j_2j_1}(p,q)$ is the inverse of the four-point propagator defined as follows:

$$I_P^{i_1i_2j_2j_1}(p,q) = \delta^{i_1j_1}\delta^{i_2j_2}(2\pi)^4\delta^4(p-q)S_q^{(-1)}(p_1)S_D^{-1}(p_2). \tag{16}$$

With this condition, we can get the normalization condition in the form

$$\begin{aligned}&-\frac{1}{6}\int \frac{d^4p}{(2\pi)^4}\{\mathrm{Tr}[\alpha_P(p_t)\beta_P(p_t)S_q(p_1)(\lambda_1\not{\varepsilon})S_q(p_1)S_D(p_2)]\\ &\quad + \mathrm{Tr}[\alpha_P(p_t)\beta_P(p_t)(2\lambda_2p_2\cdot\varepsilon)S_q(p_1)S_D^2(p_2)]\} = 1,\end{aligned} \tag{17}$$

where $\varepsilon = (1, \vec{0})$ and we define $\alpha_P(p_t)$ and $\beta_P(p_t)$ as

$$\alpha_P(p_t) = -iS_F(p_1)^{-1}\chi_p(p)S_D(P_2)^{-1}, \tag{18}$$

$$\beta_P(p_t) = -iS_D(p_2)^{-1}\bar{\chi}_p(p)S_F(P_1)^{-1}. \tag{19}$$

From Eqs. (18) and (19), we can derive the parametric forms of $\alpha_P(p_t)$ and $\beta_P(p_t)$ as

$$\alpha_P(p_t) = [\tilde{h}_1(p_t) + \not{p}_t\tilde{h}_2(p_t)]u(v), \tag{20}$$

$$\beta_P(p_t) = \bar{u}(v)[\tilde{h}_1(p_t) + \not{p}_t\tilde{h}_2(p_t)], \tag{21}$$

respectively, where $\tilde{h}_1(p_t)$ and $\tilde{h}_2(p_t)$ satisfy the following equations:

$$\tilde{h}_1(p_t) = \int \frac{d^3q_t}{(2\pi)^3}[(\tilde{V}_1 + 2\omega_D\tilde{V}_2F(Q^2))\tilde{f}_1(q_t) - (p_t\cdot q_t + q_t^2)\tilde{V}_2F(Q^2)\tilde{f}_2(q_t)], \tag{22}$$

$$\tilde{h}_2(p_t) = \int \frac{d^3q_t}{(2\pi)^3}\left[(\tilde{V}_1 - 2\omega_D\tilde{V}_2F(Q^2))\tilde{f}_2(q_t) - \frac{(p_t\cdot q_t + p_t^2)}{p_t^2}\tilde{V}_2F(Q^2)\tilde{f}_1(q_t)\right]. \tag{23}$$

We substitute Eqs. (22) and (23) into Eq. (17) and integrate out the longitudinal momentum p_l; then, the normalization condition can be written in the form

$$\begin{aligned}
&\frac{E}{24M\omega_q^3\omega_D^2(M-\omega_q-\omega_D)^2(M+\omega_q+w_D)^2}\int\frac{d^3p_t}{(2\pi)^3}\{[\lambda_1(m_q^2+\omega_q^2+2m_q\omega_q-p_t^2)(M+\omega_D+\omega_q)^2\omega_q\omega_D\\
&+\lambda_1(m_q^2+\omega_q^2-2m_q\omega_q-p_t^2)(M-\omega_D-\omega_q)^2\omega_q\omega_D+2\lambda_1(\omega_q+\omega_D)(\omega_q^2-m_q^2+p_t^2)(M+\omega_q+\omega_D)(M-\omega_q-\omega_D)\omega_D^2\\
&+2\lambda_2(M-\omega_q)\omega_q^2(M+\omega_q+\omega_D)^2(m_q+\omega_q)+2\lambda_2(M+\omega_q)\omega_q^2(M-\omega_q-\omega_D)^2(-m_q+\omega_q)]\tilde{h}_1^2(p_t)\\
&+[4\lambda_1\omega_Q^2\omega_D(M+\omega_Q+\omega_D)^2p_t^2+4\lambda_2\omega_Q^2(M-\omega_Q)(M+\omega_Q+\omega_D)^2p_t^2-4\lambda_2\omega_Q^2(M+w_Q)(M-\omega_Q-\omega_D)^2p_t^2\\
&-4\lambda_1(M-\omega_q-\omega_D)^2\omega_q^2\omega_Dp_t^2]\tilde{h}_1(p_t)\tilde{h}_2(p_t)+[\lambda_1\omega_q\omega_D(M+\omega_q+\omega_D)^2(2m_q\omega_q-\omega_q^2+p_t^2)p_t^2\\
&+\lambda_1\omega_Q\omega_D(M-\omega_Q-\omega_D)^2(-2m_Q\omega_Q-\omega_Q^2+p_t^2)p_t^2+2\lambda_2\omega_Q^2(M-\omega_Q)(m_Q-\omega_Q)(M+\omega_Q+\omega_D)^2p_t^2\\
&-2\lambda_2\omega_q^2(M-\omega_q-\omega_D)^2(M+\omega_q)(m_q+\omega_q)p_t^2+2\lambda_1\omega_D^2(\omega_D+\omega_q)(M-\omega_q-\omega_D)(M+\omega_q+\omega_D)(m_q^2-\omega_q^2-p_t^2)p_t^2]\tilde{h}_2^2(p_t)\}\\
&=1,
\end{aligned} \tag{24}$$

where E is the binding energy that is defined as $M = m_q + m_D + E$. We divide the domains of integrations in Eqs. (13) and (14) into n regions (n is sufficiently large), and then the integral equations turn out to be matrix equations. The BS scalar wave functions become n-dimensional vectors, and we just need to solve the eigenvalue equation $A\tilde{f}_{1(2)} = I$ (A is an $n\times n$ matrix). In our calculations, we take the constituent masses of the light quarks as $m_u = 0.33$ GeV, $m_s = 0.45$ GeV. The parameters m_D and E are constrained by the relation $m_D + E = M - m_{s(u)}$. Taking $m_p = 0.938$ GeV and $m_\Lambda = 1.116$ GeV, we have $m_D + E = 0.67$ GeV for Λ and 0.61 GeV for p. The parameter m_D cannot be determined, and hence we let it vary within some reasonable range. For Λ and p, we choose the diquark mass m_D to range from 700 to 800 MeV. With this choice for m_D, the binding energy E is negative and varies from -90 to -190 MeV. As we discussed before, κ ranges from 0.02 to 0.08 GeV^3. Then, for each m_D, we get a value of α_{seff} corresponding to a value of κ. In Tables I and II, we show the results for $m_D = 700$, 750, and 800 MeV for Λ and p.

Solving the eigenvalue equation, we obtain the numerical results for $\tilde{f}_1(p_t)$ and $\tilde{f}_2(p_t)$. The numerical results for the BS wave function depend on two parameters, m_D and κ. The results are shown in Figs. 1–4 for $s(ud)_{0,0}$ and $u(ud)_{0,0}$ with different values of m_D and κ. Figures 1 and 3 show the κ dependence of the BS wave functions for the system $s(ud)_{0,0}$ and the system $u(ud)_{0,0}$ for typical m_D, respectively. Figures 2 and 4 show their dependence on m_D for a typical value of κ. It can be seen from these figures that for

TABLE I. Values of α_{seff} for Λ with different κ and m_D.

	$\alpha_{\text{seff}}(\kappa = 0.02\ \text{GeV}^3)$	$\alpha_{\text{seff}}(\kappa = 0.04\ \text{GeV}^3)$	$\alpha_{\text{seff}}(\kappa = 0.06\ \text{GeV}^3)$	$\alpha_{\text{seff}}(\kappa = 0.08\ \text{GeV}^3)$
$m_D = 700$ MeV	0.72	0.76	0.78	0.80
$m_D = 750$ MeV	0.77	0.80	0.82	0.83
$m_D = 800$ MeV	0.82	0.83	0.85	0.86

TABLE II. Values of α_{seff} for p with different κ and m_D.

	$\alpha_{\text{seff}}(\kappa = 0.02\ \text{GeV}^3)$	$\alpha_{\text{seff}}(\kappa = 0.04\ \text{GeV}^3)$	$\alpha_{\text{seff}}(\kappa = 0.06\ \text{GeV}^3)$	$\alpha_{\text{seff}}(\kappa = 0.08\ \text{GeV}^3)$
$m_D = 700$ MeV	0.81	0.83	0.84	0.85
$m_D = 750$ MeV	0.85	0.86	0.87	0.88
$m_D = 800$ MeV	0.88	0.89	0.90	0.91

different baryons the shapes of the BS wave functions are rather similar. This arises from the approximate $SU(3)$ flavor symmetry and is to be excepted. All the wave functions decrease to zero when $|p_t|$ is larger than about 1.5 GeV because of the confinement interaction.

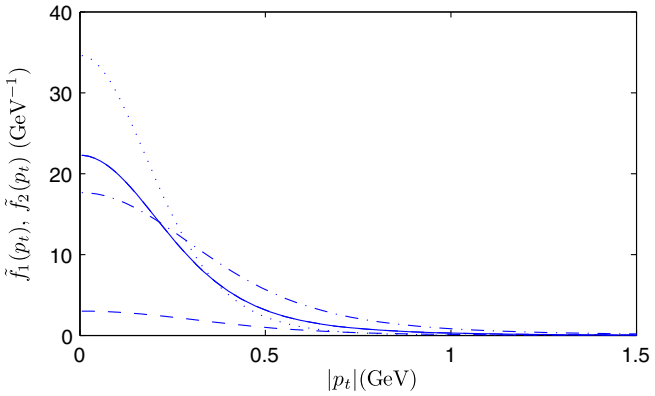

FIG. 1 (color online). The normalized BS wave functions for the system $s(ud)_{0,0}$ of Λ. When $m_D = 0.75$ GeV and $\kappa = 0.02$ GeV^3, the dotted and solid lines correspond to $\tilde{f}_1(p_t)$ and $\tilde{f}_2(p_t)$, respectively. The dashed-dotted and dashed lines correspond to $\tilde{f}_1(p_t)$ and $\tilde{f}_2(p_t)$, respectively, when $m_D = 0.75$ GeV and $\kappa = 0.08$ GeV^3.

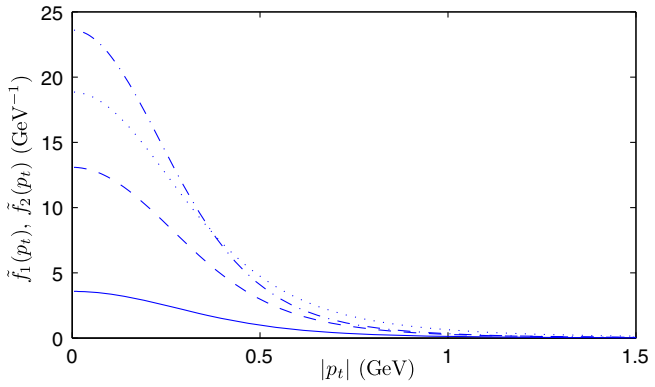

FIG. 2 (color online). The normalized BS wave functions for the system $s(ud)_{0,0}$ of Λ. When $\kappa = 0.05$ GeV^3 and $m_D = 0.7$ GeV, the dotted and solid lines correspond to $\tilde{f}_1(p_t)$ and $\tilde{f}_2(p_t)$, respectively. The dashed-dotted and dashed lines correspond to $\tilde{f}_1(p_t)$ and $\tilde{f}_2(p_t)$, respectively, when $\kappa = 0.05$ GeV^3 and $m_D = 0.8$ GeV.

III. $\Lambda_b \to \Lambda$ AND $\Lambda_b \to p$ FORM FACTORS

Based on $SU(6)$ wave functions of the proton, the proton state can be expanded in the terms of quark-diquark configurations [23]:

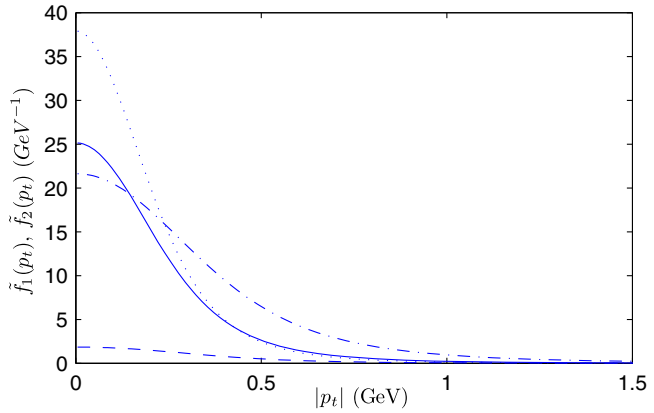

FIG. 3 (color online). The normalized BS wave functions for the system $u(ud)_{0,0}$ of p. When $m_D = 0.75$ GeV and $\kappa = 0.02$ GeV^3, the dotted and solid lines correspond to $\tilde{f}_1(p_t)$ and $\tilde{f}_2(p_t)$, respectively. The dashed-dotted and dashed lines correspond to $\tilde{f}_1(p_t)$ and $\tilde{f}_2(p_t)$, respectively, when $m_D = 0.75$ GeV and $\kappa = 0.08$ GeV^3.

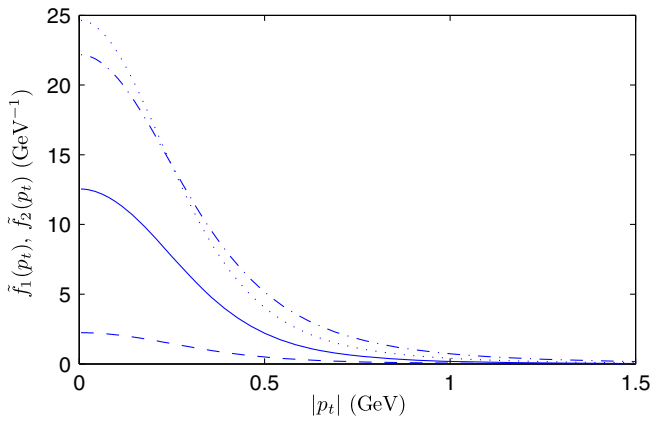

FIG. 4 (color online). The normalized BS wave functions for the system $u(ud)_{0,0}$ of p. When $\kappa = 0.05$ GeV^3 and $m_D = 0.7$ GeV, the dotted and solid lines correspond to $\tilde{f}_1(p_t)$ and $\tilde{f}_2(p_t)$, respectively. The dashed-dotted and dashed lines correspond to $\tilde{f}_1(p_t)$ and $\tilde{f}_2(p_t)$, respectively, when $\kappa = 0.05$ GeV^3 and $m_D = 0.8$ GeV.

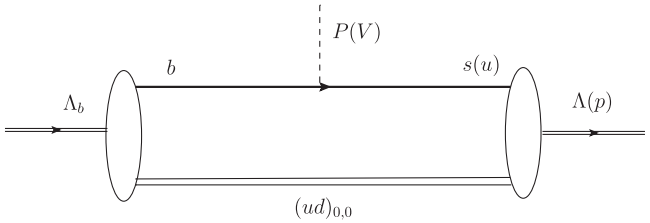

FIG. 5. $\Lambda_b \to \Lambda(p)P(V)$, where P and V are a pseudoscalar meson and a vector meson, respectively. In these transitions, $(ud)_{0,0}$ behaves as a spectator.

$$p^{\uparrow} = \frac{1}{3\sqrt{2}}[3u^{\uparrow}(ud)_{0,0} + u^{\uparrow}(ud)_{1,0} - \sqrt{2}u^{\downarrow}(ud)_{1,1} - \sqrt{2}d^{\uparrow}(uu)_{1,0} + 2d^{\downarrow}(uu)_{1,1}], \tag{25}$$

$$p^{\downarrow} = \frac{1}{3\sqrt{2}}[3u^{\downarrow}(ud)_{0,0} - u^{\uparrow}(ud)_{1,-1} + \sqrt{2}u^{\uparrow}(ud)_{1,-1} + \sqrt{2}d^{\downarrow}(uu)_{1,0} - 2d^{\uparrow}(uu)_{1,-1}]. \tag{26}$$

In the same way, we can obtain the forms of Λ [23],

$$\Lambda^{\uparrow} = \frac{1}{2\sqrt{3}}[2s^{\uparrow}(ud)_{0,0} + \sqrt{2}d^{\downarrow}(us)_{1,1} - d^{\uparrow}(us)_{1,0} + d^{\uparrow}(us)_{0,0} - \sqrt{2}u^{\downarrow}(ds)_{1,1} + u^{\uparrow}(ds)_{1,0} - u^{\uparrow}(ds)_{0,0}], \tag{27}$$

$$\Lambda^{\downarrow} = \frac{1}{2\sqrt{3}}[2s^{\downarrow}(ud)_{0,0} - \sqrt{2}d^{\uparrow}(us)_{1,-1} + d^{\downarrow}(us)_{1,0} + d^{\downarrow}(us)_{0,0} + \sqrt{2}u^{\uparrow}(ds)_{1,-1} - u^{\downarrow}(ds)_{1,0} - u^{\downarrow}(ds)_{0,0}]. \tag{28}$$

In Eqs. (25)–(28), the arrow $\uparrow$ ($\downarrow$) indicates that the spin direction of the corresponding baryon is up (down).

Λ_b is regarded as a bound state of a b quark and a scalar diquark $(ud)_{0,0}$. In the transition $\Lambda_b \to \Lambda$ (p) shown in Fig. 5, the b quark decays into the s (u) quark, and the scalar diquark behaves as a spectator.

We first study $\Lambda_b \to \Lambda$ transition, the matrix of which has the general form [10]

$$\begin{aligned}&\langle\Lambda(P',s')|\bar{s}\gamma^{\mu}b|\Lambda_b(P,s)\rangle \\ &\quad= \bar{u}_{\Lambda}(P',s')[g_1\gamma^{\mu} + ig_2\sigma^{\mu\nu}q_{\nu} + g_3q^{\mu}]u_{\Lambda_b}(P,s), \\ &\langle\Lambda(P',s')|\bar{s}\gamma^{\mu}\gamma_5 b|\Lambda_b(P,s)\rangle \\ &\quad= \bar{u}_{\Lambda}(P',s')[t_1\gamma^{\mu} + it_2\sigma^{\mu\nu}q_{\nu} + t_3q^{\mu}]\gamma_5 u_{\Lambda_b}(P,s),\end{aligned} \tag{29}$$

where $q = P - P'$ and the form factors g_i and t_i $(i = 1,2,3)$ are functions of q^2. The most general form for the matrix element in Eq. (29) consistent with the spin symmetry on the b quark in the limit $m_b \to \infty$ is

$$\begin{aligned}&\langle\Lambda(P',s')\bar{s}\gamma^{\mu}(1-\gamma_5)b\Lambda_b(v,s)\rangle \\ &\quad= \bar{u}_{\Lambda}(P',s')(F_1 + F_2\not{v})\gamma^{\mu}(1-\gamma_5)u_{\Lambda_b}(v,s),\end{aligned} \tag{30}$$

where F_i $(i = 1,2)$ are functions of $v \cdot P'$, and we have used the constraints

$$\not{v}u_{\Lambda_b}(v,s) = u_{\Lambda_b}(v,s), \qquad \not{P}'u_{\Lambda}(p',s') = Mu_{\Lambda}(p',s'). \tag{31}$$

Comparing Eq. (30) with Eq. (29), we obtain the following relations:

$$\begin{aligned}g_1 = t_1 &= \left(F_1 + \frac{M_{\Lambda}}{M_{\Lambda_b}}F_2\right), \\ g_2 = g_3 = t_2 = t_3 &= \frac{1}{M_{\Lambda_b}}F_2.\end{aligned} \tag{32}$$

In the second section, we have obtained the BS wave functions of the $s(ud)_{0,0}$ $[u(ud)_{0,0}]$ configuration of $\Lambda(p)$. The BS wave function of Λ_b was given in previous works and has the form $\chi_P^{\Lambda_b}(p) = \phi^{\Lambda_b}(p)u_{\Lambda_b}(v,s)$, where $\phi^{\Lambda_b}(p)$ is the scalar BS wave function [17,19]. The transition matrix for $\Lambda_b \to \Lambda$ can be expressed in terms of the BS wave function of Λ_b and the $s(ud)_{0,0}$ component of Λ,

$$\begin{aligned}&\langle\Lambda(P',s')\bar{s}\gamma_{\mu}(1-\gamma_5)b\Lambda_b(P,s)\rangle \\ &\quad= \int\frac{d^4p}{(2\pi)^4}\bar{\chi}_{P'}^{\Lambda}(p')\gamma_{\mu}(1-\gamma_5)\chi_P^{\Lambda_b}(p)S_D^{-1}(p_2),\end{aligned} \tag{33}$$

where $\chi_{P'}^{\Lambda}(p')$ represents the BS wave function of the $s(ud)_{0,0}$ component. On the grounds of Lorentz invariance, we define the following equation:

$$\int\frac{d^4p}{(2\pi)^4}f_2(p')p'_{t\nu}\phi^{\Lambda_b}(p)S_D^{-1}(p_2) = l_1v_{\nu} + l_2v'_{\nu}. \tag{34}$$

Considering $p_{t\nu}\cdot v_{\nu} = 0$, $p'_{t\nu}\cdot v'^{\nu} = 0$ and $v^2 = v'^2 = 1$, we can get

$$l_1 = \frac{1}{1-\omega^2}\int\frac{d^4p}{(2\pi)^4}f_2(p')p'_t\cdot v\phi^{\Lambda_b}(p)(p_l^2 - \omega_D^2), \tag{35}$$

$$l_2 = -\omega l_1. \tag{36}$$

From Eqs. (27) and (28), we can see that the Clebsch–Gordan coefficient of the $s(ud)_{0,0}$ configuration is $1/\sqrt{3}$.

Comparing Eqs. (30) and (33) and making use of Eqs. (34), (35), and (36), we can obtain the form factors for $\Lambda_b \to \Lambda$ as the following:

$$F_1 = \frac{-i}{\sqrt{3}}\int \frac{d^4p}{(2\pi)^4}\left\{f_1^\Lambda(p')\phi^{\Lambda_b}(p)S_D^{-1}(p_2) - \frac{\omega}{1-\omega^2}f_2^\Lambda(p')p_t'\cdot v\phi^{\Lambda_b}(p)(p_l^2-\omega_D^2)\right\}, \quad (37)$$

$$F_2 = \frac{-i}{\sqrt{3}}\int \frac{d^4p}{(2\pi)^4}\left\{\frac{1}{1-\omega^2}f_2^\Lambda(p')p_t'\cdot v\phi^{\Lambda_b}(p)(p_l^2-\omega_D^2)\right\}. \quad (38)$$

Substituting Eqs. (4), (8), (10), and (12) into Eq. (3) and integrating q_l, we get the relations between $f_1^\Lambda(p')$, $f_2^\Lambda(p')$ and $\tilde{f}_1^\Lambda(p_t')$, $\tilde{f}_2^\Lambda(p_t')$,

$$\begin{aligned} f_1^\Lambda(p') = {} & \frac{i}{(\lambda_1 M + p_l' - \omega_s + i\epsilon)((\lambda_2 M - p_l')^2 - \omega_D^2 - i\epsilon)}\int\frac{d^3q_t}{(2\pi)^3} \\ & \times\{[(\tilde{V}_1(p_t'-q_t)+2(p_l'-\omega_D)\tilde{V}_2(p_t'-q_t)F(Q^2))(m_s+\omega_s') - (p_t'\cdot q_t + p_t'^2)\tilde{V}_2(p_t'-q_t)F(Q^2)]\tilde{f}_1^\Lambda(q_t) \\ & + [(\tilde{V}_1(p_t'-q_t)-2(p_l'-\omega_D)\tilde{V}_2(p_t'-q_t)F(Q^2)) - (m_s+\omega_s')(p_t'\cdot q_t + p_t'^2)\tilde{V}_2F(Q^2)]\tilde{f}_2^\Lambda(q_t)\}, \end{aligned} \quad (39)$$

$$\begin{aligned} f_2^\Lambda(p') = {} & \frac{i}{(\lambda_1 M + p_l' - \omega_s + i\epsilon)((\lambda_2 M - p_l')^2 - \omega_D^2 - i\epsilon)}\int\frac{d^3q_t}{(2\pi)^3} \\ & \times\left\{\left[(\tilde{V}_1(p_t'-q_t)+2(p_l'-\omega_D)\tilde{V}_2(p_t'-q_t)F(Q^2)) - (m_s-\omega_s')\left(\tilde{V}_1(p_t'-q_t)+\frac{p_t'\cdot q_t}{p_t'^2}\tilde{V}_2(p_t'-q_t)F(Q^2)\right)\right]\tilde{f}_1^\Lambda(q_t)\right. \\ & \left. + \left[(m_s-\omega_s')(\tilde{V}_1(p_t'-q_t)-2(p_l'-\omega_D)\tilde{V}_2(p_t'-q_t)F(Q^2))\frac{p_t'\cdot q_t}{p_t'^2} - (p_t'\cdot q_t + p_t'^2)\tilde{V}_2(p_t'-q_t)F(Q^2)\right]\tilde{f}_2^\Lambda(q_t)\right\}, \end{aligned} \quad (40)$$

where $\omega_s = \sqrt{m_s^2 - p_t^2}$, $\omega_s' = \sqrt{m_s^2 - p_t'^2}$, $p_t'(= p' - p_l'\cdot v)$ and $p_l'(= p'\cdot v)$ are the transverse and longitudinal relative momenta along the momentum of Λ, respectively. Substituting Eqs. (39) and (40) and the relation between $\phi^{\Lambda_b}(p)$ and $\tilde{\phi}^{\Lambda_b}(p_t)$ [15] into Eqs. (37) and (38) and integrating out the longitudinal momentum p_l, we obtain the forms for F_1 and F_2,

$$\begin{aligned} F_1 = {} & \frac{1}{\sqrt{3}}\int\frac{d^3p_t}{(2\pi)^3}\tilde{\phi}^{\Lambda_b}(p_t)\int\frac{d^3k_t}{(2\pi)^3}\left\{-\frac{1}{2\omega_s'(M_\Lambda - \omega\omega_D - \omega_s' - \sqrt{\omega^2-1}\cos\theta p_t)}\right. \\ & \times\{[(\tilde{V}_1(p_t'-k_t)+2\omega_D\tilde{V}_2(p_t'-k_t)F(Q^2))(m_s+\omega_s') - (p_t'\cdot k_t + p_t'^2)\tilde{V}_2(p_t'-k_t)F(Q^2)]\tilde{f}_1^\Lambda(k_t) \\ & + [(\tilde{V}_1(p_t'-k_t)-2\omega_D\tilde{V}_2(p_t'-k_t)F(Q^2)) - (m_s+\omega_s')(p_t'\cdot k_t + p_t'^2)\tilde{V}_2F(Q^2)]\tilde{f}_2^\Lambda(k_t)\} \\ & + \frac{\omega}{1-\omega^2}\frac{1}{2\omega_s'(M_\Lambda - \omega\omega_D - \omega_s' - \sqrt{\omega^2-1}\cos\theta p_t)}v\cdot p_t' \\ & \times\left\{\left[(\tilde{V}_1(p_t'-k_t)+2\omega_D\tilde{V}_2(p_t'-k_t)F(Q^2)) - (m_s-\omega_s')\left(\tilde{V}_1(p_t'-k_t)+\frac{p_t'\cdot k_t}{p_t'^2}\tilde{V}_2(p_t'-k_t)F(Q^2)\right)\right]\tilde{f}_1^\Lambda(k_t)\right. \\ & \left.\left. + \left[(m_s-\omega_s')(\tilde{V}_1(p_t'-k_t)-2\omega_D\tilde{V}_2(p_t'-k_t)F(Q^2))\frac{p_t'\cdot k_t}{p_t'^2} - (p_t'\cdot k_t + p_t'^2)\tilde{V}_2(p_t'-k_t)F(Q^2)\right]\tilde{f}_2^\Lambda(k_t)\right\}\right\}, \end{aligned} \quad (41)$$

$$\begin{aligned} F_2 = {} & \frac{1}{\sqrt{3}}\int\frac{d^3p_t}{(2\pi)^3}\tilde{\phi}^{\Lambda_b}(p_t)\int\frac{d^3k_t}{(2\pi)^3} - \frac{1}{1-\omega^2}\frac{1}{2\omega_s'(M_\Lambda - \omega\omega_D - \omega_s' - \sqrt{\omega^2-1}\cos\theta p_t)}v\cdot p_t' \\ & \times\left\{\left[(\tilde{V}_1(p_t'-k_t)+2\omega_D\tilde{V}_2(p_t'-k_t)F(Q^2)) - (m_s-\omega_s')\left(\tilde{V}_1(p_t'-k_t)+\frac{p_t'\cdot k_t}{p_t'^2}\tilde{V}_2F(Q^2)\right)\right]\tilde{f}_1^\Lambda(k_t)\right. \\ & \left. + \left[(m_s-\omega_s')(\tilde{V}_1(p_t'-k_t)-2\omega_D\tilde{V}_2(p_t'-k_t)F(Q^2))\frac{p_t'\cdot k_t}{p_t'^2} - (p_t'\cdot k_t + p_t'^2)\tilde{V}_2(p_t'-k_t)F(Q^2)\right]\tilde{f}_2^\Lambda(k_t)\right\}, \end{aligned} \quad (42)$$

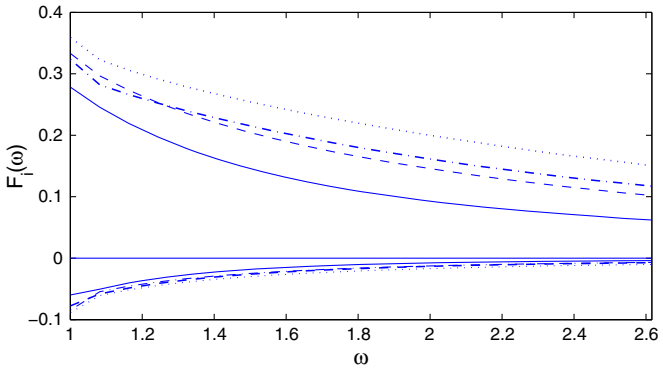

FIG. 6 (color online). $\Lambda_b \to \Lambda$ form factors F_1 (in the upper plane) and F_2 (in the lower plane) as functions of ω. The solid and dotted lines correspond to $\kappa = 0.02$ GeV^3 and 0.08 GeV^3, respectively, when $m_D = 0.75$ GeV. The dashed and dashed-dotted lines correspond to $m_D = 0.7$ GeV and $m_D = 0.8$ GeV, respectively, when $\kappa = 0.05$ GeV^3.

where $\omega = v \cdot v'$ (v and v' are the velocities of the Λ_b and Λ, respectively) is the invariant velocity transfer and θ is the angle between p_t and v_t'. All the form factors are functions of the invariant velocity transfer. $\omega = \frac{m_{\Lambda_b}^2 + m_\Lambda^2 - q^2}{2 m_{\Lambda_b} m_\Lambda}$; therefore, the minimum and maximum values of ω are 1 and $\frac{m_\Lambda^2 + m_{\Lambda_b}^2}{2 m_{\Lambda_b} m_\Lambda}$, respectively. In our calculation, we take $m_s = 0.45$ GeV, $M_\Lambda = 1.116$ GeV, and $M_{\Lambda_b} = 5.62$ GeV. Then, one can find ω ranges from 1 to 2.62. The numerical results for form factors F_1 and F_2 are plotted in Fig. 6 as functions of ω. In a similar way, we obtain the form factors for $\Lambda_b \to p$, replacing m_s by m_u and M_Λ by M_p. ω for $\Lambda_b \to p$ ranges from 1 to 3.08, and the Clebsch–Gordan coefficient of the $u(ud)_{0,0}$ configuration is $1/\sqrt{2}$. The numerical results for F_1 and F_2 are plotted in Fig. 7.

From Figs. 6 and 7, we can see that the magnitudes of form factors decrease as ω increases. This is because the overlap integrals of BS wave functions decrease with the increase of ω. We can also see that F_1 and F_2 have opposite signs and F_1 changes more rapidly than F_2 as ω increases. The numerical results of F_1 and F_2 will be used to calculate the matrix elements of $\Lambda_b \to \Lambda$ and $\Lambda_b \to p$ and the decay widths of $\Lambda_b \to \Lambda(p)P(V)$ in the next section.

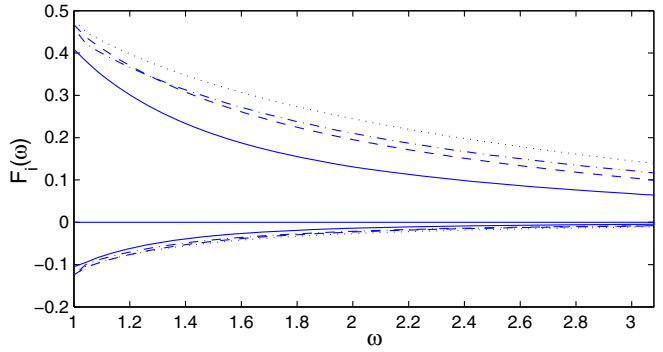

FIG. 7 (color online). $\Lambda_b \to p$ form factors F_1 (in the upper plane) and F_2 (in the lower plane) as functions of ω. The solid and dotted lines correspond to $\kappa = 0.02$ GeV^3 and 0.08 GeV^3, respectively, when $m_D = 0.75$ GeV. The dashed and dashed-dotted lines correspond to $m_D = 0.7$ GeV and $m_D = 0.8$ GeV, respectively, when $\kappa = 0.05$ GeV^3.

IV. DECAY AMPLITUDES OF Λ_b AND BRANCHING RATIOS

Based on the operator product expansion, the effective Hamiltonian $\mathcal{H}_{\rm eff}$ for the hadronic decays of Λ_b ($\Delta B = 1$) reads [24]

$$\mathcal{H}_{\rm eff} = \frac{G_F}{\sqrt{2}} \Big\{ V_{ub} V_{uq}^* [c_1(\mu) O_1^u(\mu) + c_2(\mu) O_2^u(\mu)] - V_{tb} V_{tq}^* \sum_{i=3}^{10} c_i(\mu) O_i(\mu) \Big\} + \text{H.c.}, \tag{43}$$

where $q = d, s$, G_F is the Fermi constant and $c_i(\mu)$ ($i = 1, 2, \ldots, 10$) are Wilson coefficients at the renormalization scale μ,

$$\begin{aligned} O_1^u &= (\bar{u} b)_{V-A} (\bar{q} u)_{V-A}, \\ O_2^u &= (\bar{u}_\alpha b_\beta)_{V-A} (\bar{q}_\beta u_\alpha)_{V-A}, \\ O_{3(5)} &= (\bar{q} b)_{V-A} \sum_{q'} (\bar{q}' q')_{V-A(V+A)}, \\ O_{4(6)} &= (\bar{q}_\alpha b_\beta)_{V-A} \sum_{q'} (\bar{q}'_\beta q'_\alpha)_{V-A(V+A)}, \\ O_{7(9)} &= \frac{3}{2} (\bar{q} b)_{V-A} \sum_{q'} e_{q'} (\bar{q}' q')_{V+A(V-A)}, \\ O_{8(10)} &= \frac{3}{2} (\bar{q}_\alpha b_\beta)_{V-A} \sum_{q'} e_{q'} (\bar{q}'_\beta q'_\alpha)_{V+A(V-A)}, \end{aligned} \tag{44}$$

where $O_{1,2}$ are the tree-level current-current operators, $O_{3\text{–}6}$ are the QCD penguin operators, $O_{7\text{–}10}$ are the electroweak penguin operators, $(\bar{q}_1 q_2)_{V\pm A}$ denote the usual $V \pm A$ currents, and the sum over q' runs over the quark fields that are active at the scale $\mu = O(m_b)$, i.e., $q' \in u, d, s, c, b$. The Wilson coefficients, c_i, are known to the next-to-leading logarithmic order. To be consistent, the matrix elements of the operators O_i should also be renormalized to one-loop order. The values of the effective Wilson coefficients that are renormalization scheme independent are listed in Table III [25], where k is the momentum of the gluon or photon in the penguin diagrams. First, we consider the decays of $\Lambda_b \to B_f P$ (B_f could be p or Λ, and P is a pseudoscalar meson). We note that tree operators, QCD, and the electroweak penguin operator contribute to $\Lambda_b \to p\pi^-$ and $\Lambda_b \to pK^-$, while for $\Lambda_b \to \Lambda\pi^0$, only tree and electroweak penguin operators contribute. The amplitudes for these processes can be given as [7]

TABLE III. Effective Wilson coefficients for the tree, electroweak, and QCD penguin operators.

c_i'	$k^2/m_b^2 = 0.3$	$k^2/m_b^2 = 0.5$
c_1'	1.1502	1.502
c_2'	−0.3125	−0.3125
c_3'	$2.433 \times 10^{-2} + 1.543 \times 10^{-3} i$	$2.120 \times 10^{-2} + 5.174 \times 10^{-3} i$
c_4'	$-5.808 \times 10^{-2} - 4.628 \times 10^{-3} i$	$-4.869 \times 10^{-2} - 1.552 \times 10^{-2} i$
c_5'	$1.733 \times 10^{-2} + 1.543 \times 10^{-3} i$	$1.420 \times 10^{-2} + 5.174 \times 10^{-3} i$
c_6'	$-6.668 \times 10^{-2} - 4.628 \times 10^{-3} i$	$-5.729 \times 10^{-2} - 1.552 \times 10^{-3} i$
c_7'	$-1.435 \times 10^{-4} - 2.963 \times 10^{-5} i$	$-8.340 \times 10^{-5} - 9.938 \times 10^{-5} i$
c_8'	3.389×10^{-4}	3.839×10^{-4}
c_9'	$-1.023 \times 10^{-2} - 2.963 \times 10^{-5} i$	$-1.017 \times 10^{-2} - 9.938 \times 10^{-5} i$
c_{10}'	1.959×10^{-3}	1.959×10^{-3}

$$\mathcal{M}(\Lambda_b \to p\pi^-) = i\frac{G_F}{\sqrt{2}} f_\pi \bar{u}_p(P',s')(\{V_{ub}V_{ud}^* a_1 - V_{tb}V_{td}^*[a_4 + a_{10} + (a_6 + a_8)R_1]\}[g_1(M_{\Lambda_b} - M_p) + g_3 m_\pi^2] + \{V_{ub}V_{ud}^* a_1 - V_{tb}V_{td}^*[a_4 + a_{10} + (a_6 + a_8)R_2]\}[t_1(M_{\Lambda_b} + M_p) - t_3 m_\pi^2]\gamma_5) u_{\Lambda_b}(P,s), \quad (45)$$

$$\mathcal{M}(\Lambda_b \to pK^-) = i\frac{G_F}{\sqrt{2}} f_K \bar{u}_p(P',s')(\{V_{ub}V_{us}^* a_1 - V_{tb}V_{ts}^*[a_4 + a_{10} + (a_6 + a_8)R_1]\}[g_1(M_{\Lambda_b} - M_p) + g_3 m_{K^-}^2] + \{V_{ub}V_{us}^* a_1 - V_{tb}V_{ts}^*[a_4 + a_{10} + (a_6 + a_8)R_2]\}[t_1(M_{\Lambda_b} + M_p) - t_3 m_{K^-}^2]\gamma_5) u_{\Lambda_b}(P,s), \quad (46)$$

$$\mathcal{M}(\Lambda_b \to \Lambda\pi^0) = i\frac{G_F}{2} f_\pi \bar{u}_\Lambda(P',s')\left[V_{ub}V_{us}^* a_2 - V_{tb}V_{ts}^*\left(\frac{3}{2}(a_9 - a_7)\right)\right] \times \{[g_1(M_{\Lambda_b} - M_\Lambda) + g_3 m_\pi^2] + [t_1(M_{\Lambda_b} + M_\Lambda) - t_3 m_\pi^2]\gamma_5\} u_{\Lambda_b}(P,s), \quad (47)$$

where the coefficients $a_1, a_2, \ldots, a_{10}$ are combinations of the effective Wilson coefficients after Fierz transformation, which are defined as

$$a_{2i-1} = c_{2i-1}' + \frac{1}{N_c} c_{2i}', \qquad a_{2i} = c_{2i}' + \frac{1}{N_c} c_{2i-1}', \qquad (i = 1, 2, \ldots 5), \quad (48)$$

and $R_1 = \frac{2m_P^2}{(m_b - m_u)(m_q + m_u)}$, $R_2 = \frac{2m_P^2}{(m_b + m_u)(m_1 + m_u)}$, where the quark masses are current quark masses. The most general Lorentz-invariant amplitude for the decay $\Lambda_b \to B_f P$ can be written as

$$\mathcal{M}(\Lambda_b \to B_f P) = i\bar{u}_{B_f}(P',s')(A + B\gamma_5) u_{\Lambda_b}(P,s), \quad (49)$$

where $u_{B_f}(P',s')$ is the Dirac spinors for B_f and A and B are parity-violating S-wave and parity-conserving P-wave amplitudes, respectively. The corresponding decay rate is given as [26]

$$\Gamma = \frac{p_c}{8\pi}\left\{\frac{(m_i + m_f)^2 - m_P^2}{m_i^2}|A|^2 + \frac{(m_i - m_f)^2 - m_P^2}{m_i^2}|B|^2\right\}, \quad (50)$$

where m_i, m_f, and m_P are the masses of the initial baryon, the final baryon, and the pseudoscalar meson, respectively; p_c is the c.m. momentum; and $\kappa = \frac{p_c}{E_f + m_f}$ with E_f being the energy of B_f.

Next, we consider the transition amplitudes for $\Lambda_b \to B_f V$ decay channels, where V could be ρ, K^*, and J/ψ. $\Lambda_b \to p\rho$ and pK^* receive contributions from the tree as well as QCD and electroweak penguins operators, whereas $\Lambda_b \to \Lambda\rho$ and $\Lambda J/\psi$ receive only tree and electroweak penguin operator contributions. Thus, we obtain the corresponding transition amplitudes as [7]

$$\mathcal{M}(\Lambda_b \to p\rho^-) = \frac{G_F}{\sqrt{2}} f_\rho m_\rho \epsilon^{*\mu} \bar{u}_p(P',s')[V_{ub}V_{ud}^* a_1 - V_{tb}V_{td}^*(a_4 + a_{10})]([g_1 - g_2(M_{\Lambda_b} + M_p)]\gamma_\mu + 2g_2(p_f)_\mu - \{[t_1 + t_2(M_{\Lambda_b} - M_p)]\gamma_\mu + 2t_2(p_f)_\mu\}\gamma_5) u_{\Lambda_b}(P,s), \quad (51)$$

$$\mathcal{M}(\Lambda_b \to pK^{*-}) = \frac{G_F}{\sqrt{2}} f_\rho m_K \epsilon^{*\mu} \bar{u}_p(P', s')[V_{ub}V_{us}^* a_1 - V_{tb}V_{ts}^*(a_4 + a_{10})]([g_1 - g_2(M_{\Lambda_b} + M_p)]\gamma_\mu + 2g_2(p_f)_\mu - \{[t_1 + t_2(M_{\Lambda_b} - M_p)]\gamma_\mu + 2t_2(p_f)_\mu\}\gamma_5)u_{\Lambda_b}(P, s), \quad (52)$$

$$\mathcal{M}(\Lambda_b \to \Lambda\rho^0) = \frac{G_F}{2} f_\rho m_\rho \epsilon^{*\mu} \bar{u}_\Lambda(P', s')\left[V_{ub}V_{us}^* a_2 - V_{tb}V_{ts}^* \frac{3}{2}(a_9 + a_7)\right]([g_1 - g_2(M_{\Lambda_b} + M_\Lambda)]\gamma_\mu + 2t_2(p_f)_\mu - \{[t_1 + t_2(M_{\Lambda_b} - M_\Lambda)]\gamma_\mu + 2t_2(p_f)_\mu\}\gamma_5)u_{\Lambda_b}(P, s), \quad (53)$$

$$\mathcal{M}(\Lambda_b \to \Lambda J/\psi) = \frac{G_F}{\sqrt{2}} f_{J_\psi} m_{J_\psi} \epsilon^{*\mu} \bar{u}_\Lambda(P', s')[V_{cb}V_{cs}^* a_2 - V_{tb}V_{ts}^*(a_3 + a_5 + a_7 + a_9)]([g_1 - g_2(M_{\Lambda_b} + M_\Lambda)]\gamma_\mu + 2g_2(p_f)_\mu - \{[t_1 + t_2(M_{\Lambda_b} - M_\Lambda)]\gamma_\mu + 2t_2(p_f)_\mu\}\gamma_5)u_{\Lambda_b}(P, s), \quad (54)$$

where ϵ^μ is the polarization vector of the emitted vector meson. For the $\Lambda_b \to B_f V$ decay mode, the general form for the amplitude is

$$\mathcal{M}(\Lambda_b \to B_f V) = \bar{u}_{B_f}(P', s')\epsilon^{*\mu}[A_1\gamma_\mu\gamma_5 + A_2(p_f)_\mu\gamma_5 + B_1\gamma_\mu + B_2(p_f)_\mu]u_{\Lambda_b}(P, s). \quad (55)$$

The corresponding decay rate is given as [7]

$$\Gamma = \frac{p_c}{8\pi}\frac{E_f + m_f}{m_i}\left\{2(|S|^2 + |P_2|^2) + \frac{E_V^2}{m_V^2}(|S + D|^2 + |P_1|^2)\right\}, \quad (56)$$

where $m_V(E_V)$ is the mass (energy) of the vector meson V, and

$$S = -A_1,$$
$$D = -\frac{p_c^2}{E_V(E_f + m_f)}(A_1 - m_i A_2),$$
$$P_1 = \frac{p_c}{E_V}\left(\frac{m_i + m_f}{E_f + m_f}B_1 + m_i B_2\right),$$
$$P_2 = \frac{p_c}{E_f + m_f}B_1. \quad (57)$$

N_c includes the nonfactorizable effects that are model and process dependent and cannot be theoretically evaluated accurately. Therefore, we choose to determine the values of N_c by experiment. Since the nonfactorization information included in N_c may be decay-channel dependent, the value of N_c may be different for different decay channels. This difference will be ignored due to our lack of knowledge about different decay-channel dependence. Furthermore, the nonfactorizable contribution can be absorbed into the effective parameters a_i after the Fierz transformation with ζ_i describing the nonfactorizable effects, which is defined as $1/(N_c)_i = 1/3 + \zeta_i$, and may be different for each operator. However, since we do not have enough information about the operator dependence of ζ_i, we assume ζ_i is universal for each operator, and hence we use that $(N_c)_i = N_c$. N_c, as the effective number of colors, is treated as a free parameter modeling the nonfactorizable contribution to the matrix elements, and its value can be extracted from the experimental data for the two body nonleptonic B decays. The analysis of $B \to D\pi$ data leads to $N_c \sim 2$ [27]. On the other hand, Mannel and Roberts used $N_c = \infty$ to study nonleptonic decays of Λ_b. The dominant contributions come from the coefficients a_1 and a_2 for current-current amplitudes, a_4 and a_6 for QCD penguin induced amplitudes, and a_9 for electroweak penguin induced amplitudes. It can be seen that the coefficients a_1, a_4, a_6, and a_9 are not sensitive to N_c, whereas other coefficients depend on N_c strongly. For the decays of which amplitudes depend mainly on

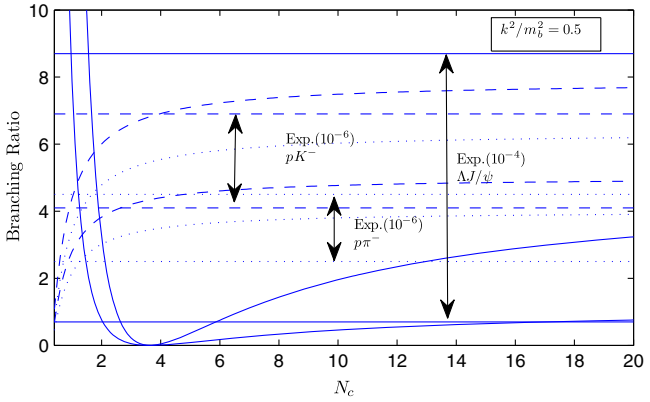

FIG. 8 (color online). Branching ratios as a function of N_c when $k^2/m_b^2 = 0.5$. In our calculation, the upper (lower) curved solid line corresponds to the upper (lower) boundary of the branching ratio of $\Lambda_b \to \Lambda J/\psi$, the upper (lower) curved dashed line corresponds to the upper (lower) boundary of the branching ratio of $\Lambda_b \to pK^-$, and the upper (lower) curved dotted line corresponds to the upper (lower) boundary of the branching ratio of $\Lambda_b \to p\pi^-$. The upper and lower horizontal solid, dashed, and dotted lines correspond to the ranges of the experimental results for $\Lambda_b \to \Lambda J/\psi$, $\Lambda_b \to pK^-$, and $\Lambda_b \to p\pi^-$.

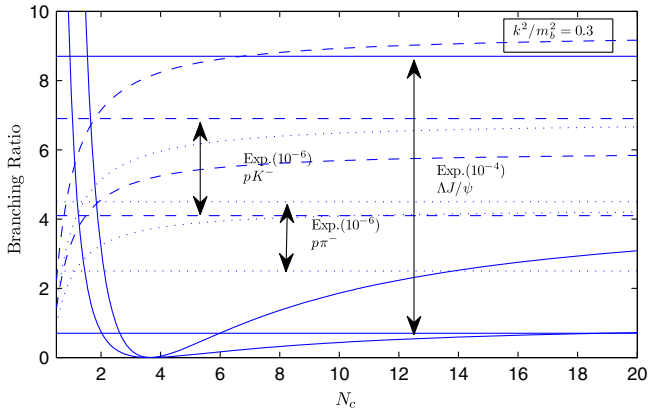

FIG. 9 (color online). Branching ratios as a function of N_c when $k^2/m_b^2 = 0.3$. In our calculation, the upper (lower) curved solid line corresponds to the upper (lower) boundary of the branching ratio of $\Lambda_b \to \Lambda J/\psi$, the upper (lower) curved dashed line corresponds to the upper (lower) boundary of the branching ratio of $\Lambda_b \to pK^-$, and the upper (lower) curved dotted line corresponds to the upper (lower) boundary of the branching ratio of $\Lambda_b \to p\pi$. The upper and lower horizontal solid, dashed, and dotted lines correspond to the ranges of the experimental results for $\Lambda_b \to \Lambda J/\psi$, $\Lambda_b \to pK^-$, and $\Lambda_b \to p\pi^-$.

N_c-insensitive coefficients, their decay rates can be reliably predicted within the factorization approach even in the absence of the information on nonfactorizable effects.

Numerically, the parameters appearing in the decay widths and the masses and decay constants of mesons are taken to have the following values [4,7]: $G_F = 1.16637 \times 10^{-5}$ GeV^{-2}, $m_{\pi^-} = 0.1396$ GeV, $m_{\pi^0} = 0.135$ GeV, $m_{K^-} = 0.4936$ GeV, $m_{K^*} = 0.892$ GeV, $m_{\rho^-} = 0.775$ GeV, $m_{J/\psi} = 3.096$ GeV, $f_\pi = 130.7$ MeV, $f_K = 159.8$ MeV, $f_{K^*} = 221$ MeV, $f_\rho = 221$ MeV, $f_{J/\psi} = 0.395$ GeV, and $\tau(\Lambda_b) = (1.425 \pm 0.032) \times 10^{-12}$ s. The CKM matrix, which should be determined from experimental data, has the following form in terms of the Wolfenstein parameters, A, λ, ρ, and η [4]:

$$\begin{pmatrix} 1-\frac{1}{2}\lambda^2 & \lambda & A\lambda^3(\rho - i\eta) \\ -\lambda & 1-\frac{1}{2}\lambda^2 & A\lambda^2 \\ A\lambda^3(1-\rho-i\eta) & -A\lambda^2 & 1 \end{pmatrix}. \quad (58)$$

We use $\lambda = 0.2235$, $A = 0.811$, $\rho_{\min} = 0.09$, $\rho_{\max} = 0.254$, $\eta_{\min} = 0.323$, and $\eta_{\max} = 0.442$. The results are shown in Figs. 8 and 9. In our calculation, we have several parameters: k^2, N_c, κ, m_D, and the CKM matrix elements. When $k^2/m_b^2 = 0.5(0.3)$, we let κ range from 0.02 to 0.08 GeV^3 and m_D range from 0.7 to 0.8 MeV. In the allowed ranges of m_D, κ, and the CKM matrix elements, we can get the upper and lower boundaries of branching ratios as a function of N_c. Then, with the experimental data for the branching ratios of the decays $\Lambda_b \to \Lambda J/\psi$, $\Lambda_b \to p\pi^-$, and $\Lambda_b \to pK^-$, we extract the allowed range for N_c from the comparison of the theoretical results and the experimental data. We exclude the ranges of N_c in which the entire calculated band lies outside the experimental band for every decay channel. As we can see from Fig. 8 ($k^2/m_b^2 = 0.5$), for $\Lambda_b \to p\pi^-$, the intersection of the upper boundary of calculation results and the smallest experimental value corresponds to $N_c = 0.62$, and the lower boundary of calculation results cannot reach the biggest value of experiment when $N_c \sim \infty$. Therefore, we should exclude $N_c < 0.62$ and obtain the range of N_c as $[0.62, \infty)$. In a similar way, we get the range of N_c as $[0.70, \infty)$ from $\Lambda_b \to pK^-$. As for the decay $\Lambda_b \to \Lambda J\psi$, the lower calculation boundary intersects with the biggest experimental result at the point $N_c = 0.98$, and the upper calculation boundary intersects with the smallest experimental result when $N_c = 2.65, 6.08$. Therefore, we should exclude $N_c < 0.98$ and $2.65 < N_c < 6.08$ and get the range of N_c as $[0.98, 2.65] \cup [6.08, \infty)$. Then, we obtain the overlap of the ranges of N_c from the three decay channels as $[0.98, 2.65] \cup [6.08, \infty)$ ($k^2/m_b^2 = 0.5$). Similarly, from Fig. 9 ($k^2/m_b^2 = 0.3$), we obtain the range of N_c as $[0.95, 2.63] \cup [5.98, \infty)$. We can see that the decay $\Lambda_b \to \Lambda J/\psi$ plays the main role in limiting the range of N_c. This is because the decay amplitude of $\Lambda_b \to \Lambda J/\psi$ includes coefficients a_2, a_3, a_5, and a_7, which are sensitive to N_c, while for $\Lambda_b \to p\pi^-$ and $\Lambda_b \to pK^-$, their amplitudes depend mainly on other coefficients (a_1, a_4, and a_6) that are insensitive to N_c. Then, we can give the predictions for the branching ratios of the decays $\Lambda_b \to \Lambda\pi^0(\rho^0)$ and $\Lambda_b \to p\rho^-(K^*)$. The numerical results are shown in Tables IV and V. These predictions will be tested in future experiments.

TABLE IV. The smallest/biggest predicted values of branching ratios for $\Lambda_b \to \Lambda\pi^0$, $\Lambda\rho$, $p\rho^-$, and pK^* in the obtained ranges of N_c when $q^2/m_b^2 = 0.3$. The uncertainties when N_c takes the limiting values are caused by the uncertainties of m_D and κ.

Decay processes	$N_c \in [0.95, 2.62]$	$N_c \in [5.98, \infty)$
$\Lambda_b \to \Lambda\rho^0(10^{-8})$	$1.13 \sim 1.72/7.76 \sim 11.49$	$1.56 \sim 2.11/10.68 \sim 13.86$
$\Lambda_b \to \Lambda\pi^0(10^{-8})$	$0.81 \sim 1.31/7.97 \sim 10.67$	$1.07 \sim 1.43/7.97 \sim 10.67$
$\Lambda_b \to pK^*(10^{-6})$	$1.75 \sim 2.76/4.05 \sim 6.37$	$3.31 \sim 3.43/7.22 \sim 7.93$
$\Lambda_b \to p\rho^-(10^{-6})$	$1.61 \sim 2.40/3.68 \sim 5.50$	$2.87 \sim 3.15/6.23 \sim 7.20$

TABLE V. The smallest/biggest predicted values of branching ratios for $\Lambda_b \to \Lambda\pi^0$, $\Lambda\rho$, $p\rho^-$, and pK^* in the obtained ranges of N_c when $q^2/m_b^2 = 0.5$. The uncertainties when N_c takes the limiting values are caused by the uncertainties of m_D and κ.

Decay processes	$N_c \in [0.98, 2.65]$	$N_c \in [6.08, \infty)$
$\Lambda_b \to \Lambda\rho^0(10^{-8})$	$1.45 \sim 2.27/7.62 \sim 11.20$	$1.99 \sim 2.68/10.45 \sim 13.65$
$\Lambda_b \to \Lambda\pi^0(10^{-8})$	$1.04 \sim 1.61/5.97 \sim 9.23$	$1.39 \sim 1.85/8.02 \sim 10.66$
$\Lambda_b \to pK^*(10^{-6})$	$2.11 \sim 3.29/4.87 \sim 7.60$	$3.74 \sim 4.11/8.63 \sim 9.47$
$\Lambda_b \to p\rho^-(10^{-6})$	$1.58 \sim 2.41/3.59 \sim 5.52$	$2.73 \sim 2.98/6.24 \sim 6.83$

V. SUMMARY AND DISCUSSION

In the quark-diquark model, a light baryon that is composed of u, d, and s quarks can be regarded as a bound state of various quark and light diquark configurations. The Clebsch–Gordan coefficients of this configurations are given based on the $SU(6)$ wave functions. With this picture, we have established the BS equation for the configuration including a scalar diquark in the light baryon. The kernel for the BS equation contains the scalar confinement and one-gluon-exchange terms, which are motivated by the potential model and successfully used in the case mesons and heavy baryons containing a single heavy quark and two heavy quarks. The BS equations for Λ and p have been solved numerically under the covariant instantaneous approximation. Then, we have calculated the form factors for $\Lambda_b \to \Lambda(p)$ transitions using the obtained BS wave functions. Working in the factorization approach, we have obtained the transition amplitudes for various decay processes and consequently calculated the decay branching ratios. In the calculation of Λ_b decays, the Wilson coefficients for the tree and penguin operators at the scale m_b are involved. We have used the renormalization-scheme-independent Wilson coefficients. One of the major uncertainties in our calculations is the effective parameter N_c. We have compared theoretical results for the branching ratios of $\Lambda_b \to \Lambda J/\psi$, $\Lambda_b \to p\pi^-$, and $\Lambda_b \to pK^-$ with experimental results and extracted allowed ranges for N_c, within which we have obtained the predictions for the branching ratios of $\Lambda_b \to \Lambda\rho^0(\pi^0)$ and $\Lambda_b \to pK^*(\rho^-)$. It should be noted that the decay modes $\Lambda_b \to \Lambda\pi^0$ and $\Lambda_b \to \Lambda\rho^0$ have the smallest branching ratios in comparison to others. This is because these decay modes are suppressed by the CKM matrix elements and receive contributions from a_2, which are smaller. Furthermore, in these two decay modes, besides tree operator contributions, there are only electroweak penguin operator contributions that are believed to be smaller compared to those of QCD penguin operators because of the smallness of electroweak Wilson coefficients. Thus, the branching ratios of $\Lambda_b \to \Lambda\pi^0$ and $\Lambda_b \to \Lambda\rho^0$ in our model are expected to be two orders smaller than those of $\Lambda_b \to p\pi^-, p\rho^-$, pK^-, and pK^* decays.

ACKNOWLEDGMENTS

This work is supported by the National Natural Science Foundation of China (Projects No. 11175020 and No. 11275025).

[1] J. Abdallah *et al.*, Phys. Lett. B **585**, 63 (2004).
[2] A. Abulencia *et al.*, Phys. Rev. Lett. **98**, 122002 (2007).
[3] F. Abe *et al.*, Phys. Rev. D **55**, 1142 (1997).
[4] J. Beringer *et al.* (Particle Data Group), Phys. Rev. D **86**, 010001 (2012).
[5] V. M. Abazov *et al.*, Phys. Rev. D **84**, 031102 (2011).
[6] H.-Y. Cheng, Phys. Rev. D **56**, 2799 (1997).
[7] R. Mohanta, A. K. Giri, and M. P. Khanna, Phys. Rev. D **63**, 074001 (2001).
[8] O. Leitner, Z. J. Ajaltouni, and E. Conte, arXiv:hep-ph/0602043v1.
[9] X.-H. Guo, A. W. Thomas, and A. G. Williams, Phys. Rev. D **59**, 116007 (1999).
[10] W. Roberts, Phys. Lett. B **282**, 453 (1992); Nucl. Phys. **B389**, 549 (1993); A. Datta, Phys. Lett. B **349**, 348 (1995).
[11] X.-H. Guo, T. Huang, and Z.-H. Li, Phys. Rev. D **53**, 4946 (1996).
[12] E. E. Salpeter and H. S. Bethe, Phys. Rep. **200**, 127 (1991).
[13] N. Nakanishi, Prog. Theor. Phys. Suppl. **43**, 1 (1969).
[14] M.-H. Weng, X.-H. Guo, and A. W. Thomas, Phys. Rev. D **83**, 056006 (2011).
[15] X.-H. Guo and T. Muta, Phys. Rev. D **54**, 4629 (1996).
[16] L. Zhang and X.-H. Guo, Phys. Rev. D **87**, 076013 (2013).
[17] E. Eichten, K. Gottfried, T. Kinoshita, K. D. Lane, and T.-M. Yan, Phys. Rev. D **17**, 3090 (1978).
[18] M. Anselmino, P. Kroll, and B. Pire, Z. Phys. C **36**, 89 (1987).

[19] X.-H. Guo and H.-K. Wu, Phys. Lett. B **654**, 97 (2007).
[20] X.-H. Guo and X.-H. Wu, Phys. Rev. D **76**, 056004 (2007).
[21] X.-H. Guo, K.-W. Wei, and X.-H. Wu, Phys. Rev. D **77**, 036003 (2008).
[22] H.-Y. Jin, C.-S. Huang, and Y.-B. Dai, Z. Phys. C **56**, 707 (1992); Y.-B. Dai, C.-S. Huang, and H.-Y. Jin, Z. Phys. C **60**, 527 (1993); Y.-B. Dai, C.-S. Huang, and H.-Y. Jin, Phys. Lett. B **331**, 174 (1994); C.-H. Chang, C.-S. Huang, and G.-L. Wang, Commun. Theor. Phys. **44**, 646 (2005).
[23] C. Boros and A. W. Thomas, Phys. Rev. D **60**, 074017 (1999).
[24] G. Buchalla, A. J. Buras, and M. E. Lautenbacher, Rev. Mod. Phys. **68**, 1125 (1996).
[25] X.-H. Guo, O. Leitner, and A. W. Thomas, Phys. Rev. D **63**, 056012 (2001).
[26] S. F. Tuan and S. P. Rosen, Phys. Rev. D **51**, 6259 (1995); S. Pakvasa, S. F. Tuan, and S. P. Rosen, Phys. Rev. D **42**, 3746 (1900).
[27] H. Y. Cheng and K. C. Yang, Phys. Rev. D **59**, 092004 (1999).